universe

MDPI

Communication

Detecting Wandering Intermediate-Mass Black Holes with AXIS in the Milky Way and Local Massive Galaxies

Fabio Pacucci [1,2,*], Bryan Seepaul [1], Yueying Ni [1], Nico Cappelluti [3] and Adi Foord [4]

[1] Center for Astrophysics | Harvard & Smithsonian, 60 Garden St., Cambridge, MA 02138, USA
[2] Black Hole Initiative, Harvard University, 20 Garden St., Cambridge, MA 02138, USA
[3] Department of Physics, University of Miami, 1320 Campo Sano Ave, Coral Gables, FL 33146, USA
[4] Department of Physics, University of Maryland Baltimore County, 1000 Hilltop Cir, Baltimore, MD 21250, USA
* Correspondence: fabio.pacucci@cfa.harvard.edu

Abstract: This white paper explores the detectability of intermediate-mass black holes (IMBHs) wandering in the Milky Way (MW) and massive local galaxies, with a particular emphasis on the role of AXIS. IMBHs, ranging within $10^{3-6}\,\mathrm{M}_\odot$, are commonly found at the centers of dwarf galaxies and may exist, yet undiscovered, in the MW. By using model spectra for advection-dominated accretion flows (ADAFs), we calculated the expected fluxes emitted by a population of wandering IMBHs with masses of $10^5\,\mathrm{M}_\odot$ in various MW environments and extrapolated our results to massive local galaxies. Around 40% of the potential population of wandering IMBHs in the MW can be detected in an AXIS deep field. We proposed criteria to aid with selecting IMBH candidates using already available optical surveys. We also showed that IMBHs wandering in >200 galaxies within 10 Mpc can be easily detected with AXIS when passing within dense galactic environments (e.g., molecular clouds and cold neutral medium). In summary, we highlighted the potential X-ray detectability of wandering IMBHs in local galaxies and provided insights for guiding future surveys. Detecting wandering IMBHs is crucial for understanding their demographics and evolution and the merging history of galaxies. *This white paper is part of a series commissioned for the AXIS Probe Concept Mission; additional AXIS white papers can be found at the AXIS website.*

Keywords: intermediate-mass black holes; X-ray surveys; galaxy; black hole physics

check for updates

Citation: Pacucci, F.; Seepaul, B.; Ni, Y.; Cappelluti, N.; Foord, A. Detecting Wandering Intermediate-Mass Black Holes with AXIS in the Milky Way and Local Massive Galaxies. *Universe* **2024**, *10*, 225. https://doi.org/10.3390/universe10050225

Academic Editor: Taotao Fang

Received: 12 April 2024
Revised: 2 May 2024
Accepted: 13 May 2024
Published: 17 May 2024

Copyright: © 2024 by the authors. Licensee MDPI, Basel, Switzerland. This article is an open access article distributed under the terms and conditions of the Creative Commons Attribution (CC BY) license (https://creativecommons.org/licenses/by/4.0/).

1. Introduction

Many of the black holes (BHs) observed thus far are accreting at or near the Eddington rate $\dot{M}_{\mathrm{Edd}} \approx 1.4 \times 10^{18} M_\bullet\,\mathrm{g\,s^{-1}}$, where $M_\bullet$ is the mass of the compact object in solar masses. In this limiting case, the outward acceleration on a test particle resulting from radiation pressure is balanced by the inward gravitational acceleration. Notably, this is the case for high-luminosity quasars, which are characterized by super-massive BHs with masses $M_\bullet > 10^6\,\mathrm{M}_\odot$. In the conventional α-disk model [1,2], ∼10% of the rest-mass energy (Mc^2) of the infalling material is radiated away [3].

This standard picture of accretion has been widely tested, especially in the high-z Universe [4], where the large availability of gas makes accretion at the Eddington rate feasible [5]. However, the radiative efficiency, ϵ, can significantly deviate from the typical 10% value, both for strongly super-Eddington ($\dot{M} \gg \dot{M}_{\mathrm{Edd}}$) and sub-Eddington ($\dot{M} \ll \dot{M}_{\mathrm{Edd}}$) accretion rates [6–10]. For accretion rates in the range $0.01\dot{M}_{\mathrm{Edd}} < \dot{M} < \dot{M}_{\mathrm{Edd}}$, the accreting material creates a radiatively efficient, geometrically thin and optically thick accretion disk [1]. The radiative efficiency in this particular case depends on the spin of the black hole and varies from ∼6% for non-rotating black holes to ∼32% for maximally rotating ones [11]; hence, it is ∼10% on average.

Below 1% of the Eddington rate, theoretical calculations suggest that the flow enters the regime of advection-dominated accretion flow (ADAF) [12–16]. BHs accreting in

ADAF mode exhibit radiative efficiencies several orders of magnitude lower than the typical ∼10% value. Given the rarity of conditions supporting large accretion rates in the local Universe, it is likely that a substantial fraction of BHs accretes in the ADAF mode, e.g., the super-massive BH at the center of the MW [17]. Similarly, a putative population of intermediate-mass BHs (IMBHs) wandering in galaxies would also accrete in ADAF mode. It is important to note that, while accretion processes characterized by rates lower than 1% of the Eddington rate are typically denominated ADAF, the specifics of the accretion flow and its effects on the environment (e.g., the possibility of forming a jet, see Tchekhovskoy et al. [18]) depend on environmental properties (e.g., its density) and on the evolutionary history of the system.

IMBHs are a bridge between stellar mass and super-massive objects and have masses in the range $10^3\,\mathrm{M}_\odot < M_\bullet < 10^6\,\mathrm{M}_\odot$, although the definition greatly varies depending on the sub-field of interest. Central IMBHs have been extensively detected in dwarf galaxies; their mass generally follows the scaling relations between black hole mass and stellar mass [19]. Additionally, dwarf galaxies have active fractions ranging from ∼5% to 22% [20,21]. Some of these central black holes in dwarf galaxies, and up to $z \sim 3$, are found to be significantly overmassive with respect to the stellar content of their hosts, in violation of scaling relations [22,23]. Exceptionally overmassive black holes are now systematically found in the high-z Universe [24,25] by JWST. The redshift evolution of these populations of black holes and the role that wandering black holes played in their formation (see, e.g., [26]) is still unclear. For these reasons, recent studies are focusing on investigating the existence of wandering IMBHs in the MW and massive galaxies and their orbital and radiative properties [26–29].

IMBHs potentially wandering in the MW could have formed (i) in situ and (ii) ex situ. In situ (i.e., within the galaxy) formation channels include direct collapse of high-mass quasi-stars [30,31], super-Eddington accretion onto stellar-mass BHs [32], runaway mergers in dense globular stellar clusters [33–37], and supra-exponential accretion on seed black holes in the early Universe [38,39]. The ex situ channel forms wandering black holes through tidal disruption of satellite/dwarf galaxies when merged into larger halos [40–43].

These wandering IMBHs accrete from the interstellar medium (ISM) at low rates $\dot{M} \ll \dot{M}_{\mathrm{Edd}}$, resulting in electromagnetic signatures typical of the ADAF accretion mode. A recent study [44] modeled the accretion and radiation properties of putative IMBHs with masses of $10^5\,\mathrm{M}_\odot$ wandering in the MW using five realistic ISM environments [45]: molecular clouds (MCs), cold neutral medium (CNM), hot neutral medium (HNM), warm ionized medium (WIM), and hot ionized medium (HIM). MC is the densest environment, with typical gas number densities of 10^2–$10^4\,\mathrm{cm}^{-3}$, while HIM is the most rarified environment, with typical gas number densities of $10^{-3}\,\mathrm{cm}^{-3}$. All results presented here consider the volume fractions of the different environments considered. MC is the most uncommon environment, occupying only ∼0.05% of the volume of the MW, while HIM is the most common, with a volume occupation fraction of ∼47%: almost half of the entire volume [44]. The mass of a perturbing black hole was chosen as the typical mass of IMBHs detected in the nuclei of dwarfs [20]. The accretion rate onto the IMBH was estimated using a Bondi rate, which was adequately adjusted to account for outflows and convection [44,46–48].

This white paper first summarizes the result presented in [44], which focused on the X-ray properties of wandering IMBHs in the MW. Then, it expands on the contribution that AXIS [49] could provide to detect these sources. Lastly, it predicts the observability of IMBHs wandering in local galaxies.

2. Detecting Wandering IMBHs Using X-rays with AXIS

2.1. Accretion Rates and Spectral Energy Distributions

The left panel of Figure 1 shows the distribution of accretion rates predicted for a $10^5\,\mathrm{M}_\odot$ IMBH wandering in typical ISM environments of the MW. The accretion rates range between 10^{-14} and $10^{-4}\,\mathrm{M}_\odot\,\mathrm{yr}^{-1}$; hence, they span ∼10 orders of magnitude. MC and

CNM environments show the highest accretion rates because they are the densest; as such, they offer the best chance for X-ray detection of IMBHs in the MW.

As a reference, the Eddington rate for a $10^5\,M_\odot$ IMBH is $\dot{M}_{\rm Edd} \approx 2 \times 10^{-3}\,M_\odot\,{\rm yr}^{-1}$: all accretion rates predicted are strongly sub-Eddington. The resulting spectral energy distributions (SEDs) typical for the five ISM environments are shown in the right panel of Figure 1, with Eddington ratios (i.e., the actual accretion rate normalized to the Eddington rate) ranging from 10^{-11} to 10^{-3}. The SEDs were calculated using a code designed specifically for ADAF mode accretion [50]. The SED peak shifts to higher frequencies with increasing accretion rates.

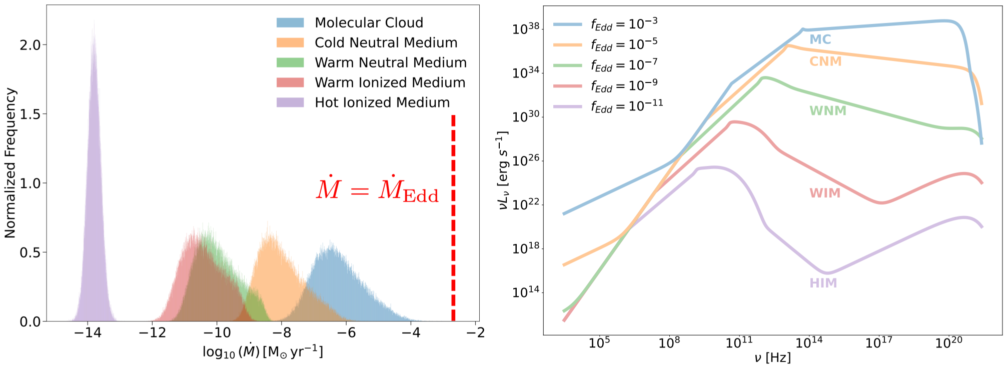

Figure 1. Left panel: distribution of accretion rates, categorized by the five ISM environments investigated. All rates are strongly sub-Eddington. **Right panel:** collection of SEDs for five values of the accretion rate representative of each ISM environment.

2.2. X-ray Observability and Selection Criteria: The Role of AXIS

The left panel of Figure 2 shows the resulting (volume-weighted) X-ray flux distribution. These results suggest that AXIS, in its proposed deep survey [51,52] with a flux limit $\sim 3 \times 10^{-18}$ erg s^{-1} cm^{-2} and an area of 0.1 deg^{-2}, will detect a fraction, in number, of $\sim$38% of wandering IMBHs in the MW, assuming a uniform sampling of the region occupied by the galaxy [49].

To aid in the task of selecting IMBH candidates, [44] proposed essential selection criteria to be used in photometric surveys. The right panel of Figure 2 shows two luminosity ratios calculated as a function of the Eddington ratio of the IMBH: (i) the X-ray-to-optical/UV ratio represented by the standard $\alpha_{\rm ox}$ parameter [53] and (ii) the optical/UV to sub-mm ratio (see [44] for their definition). A combination of X-ray, optical, and sub-mm observations can sift out potential candidates and uniquely determine the accretion rate onto wandering IMBHs.

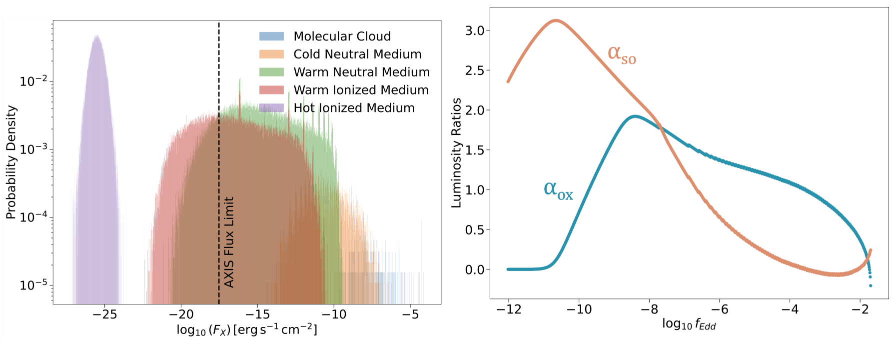

Figure 2. Left panel: Probability density of the X-ray fluxes produced by IMBHs passing through the five ISM environments considered. The AXIS flux limit is indicated. **Right panel:** Luminosity ratios (optical-to-X-ray and sub-mm-to-optical) for selecting IMBH candidates in multi-wavelength surveys.

Predicting the number of IMBHs detectable by AXIS in a deep galactic survey is challenging because the total number of such sources is unknown. The MW has encountered $\sim 15 \pm 3$ galaxies with stellar mass $> 10^7\,M_\odot$ during its cosmic evolution [54]. Such galaxies could have hosted IMBHs that are massive enough to be detected in AXIS searches. Therefore, assuming an expected number of $\sim$10 IMBHs, ref. [28] showed that these objects are more likely to wander in the innermost $\sim$1 kpc of the MW. However, it is informative to compare the capabilities of AXIS with those of other facilities that are currently operational. Table 1 shows that AXIS would allow for a significant improvement of at least 40% over current facilities, thanks not only to its extraordinary sensitivity but also to its wide field of view.

Table 1. Volume-weighted detectability of wandering IMBHs of $10^5\,M_\odot$ in the MW by AXIS, Chandra, and eROSITA. The detectability indicates the percent of the total number of objects that are detectable by a given instrument.

X-ray Telescope	Flux Limit [$\mathrm{erg\,s^{-1}\,cm^{-2}}$]	Detectability
AXIS	3.0×10^{-18}	38%
Chandra	2.0×10^{-16}	27%
eRosita	2.0×10^{-14}	13%

2.3. Extending the Search to Local Galaxies

The left panel of Figure 2 shows that the passage of a $10^5\,M_\odot$ IMBH generates the highest X-ray fluxes within MC and CNM environments. Galaxies in the same mass category of the MW share a similar environmental composition. Hence, we investigate the fluxes that the passage of equally massive IMBHs would produce in nearby galaxies.

In Figure 3, we show the X-ray fluxes (0.2–10 keV) generated by the passage of a $10^5\,M_\odot$ IMBH in the five ISM environments for a range of distances between 1 kpc and 10 Mpc. We indicate the distance to a few example locations, from the galactic center to the Andromeda galaxy, noting that within a radius of 4 Mpc, there are more than 200 galaxies, although many of them are dwarfs [55]. We calculated the flux reported in Figure 3 for the five ISM environments from their *median luminosities*. As some environments exhibit a range of luminosities spanning $\sim$13 orders of magnitudes (see Figure 2), the typical values of fluxes in Figure 3 are indicative.

From Figure 3, we see that the median luminosities generated in the WNM, WIM, and HIM are invisible to AXIS or are detectable only within the MW. On the contrary, fluxes generated in the CNM and MCs are detectable by an AXIS deep field well outside the MW. AXIS imaging reaching a depth of $\sim 3 \times 10^{-18}\,\mathrm{erg\,s^{-1}\,cm^{-2}}$ could detect the electromagnetic signature of the passage of an IMBH of $10^5\,M_\odot$ in hundreds of galaxies within 10 Mpc distance. Although MC and CNM environments occupy only a small volume fraction of a typical MW-like galaxy (0.05% and 1%, respectively; see [45]), the availability of a large number of external galaxies within reach dramatically expands the chances of detecting such signatures.

As most of the X-ray luminosities of the sources considered here are $<10^{40}\,\mathrm{erg\,s^{-1}}$, contamination from X-ray binaries (XRBs) is of concern. To disentangle their emissions, synergies with observatories that use other wavelengths (e.g., JWST, Roman, and Rubin) will be fundamental.

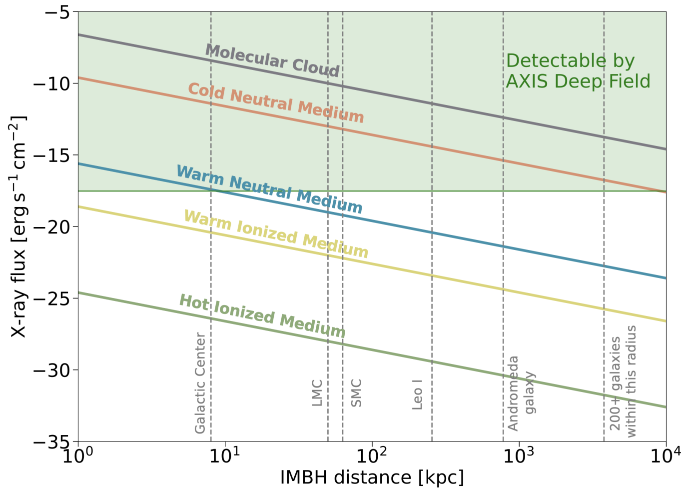

Figure 3. X-ray fluxes (0.2–10 keV) generated by the passage of a 10^5 $M_\odot$ IMBH as a function of its distance. The green-shaded area is detectable by an AXIS deep field. Electromagnetic signatures of the passage of an IMBH can be detected in MC and CNM in hundreds of galaxies within 10 Mpc.

3. Concluding Remarks

To conclude, AXIS represents a significant improvement over current X-ray facilities and opens the way to detect a completely unknown population of black holes. In the MW and, even more crucially, in >200 local galaxies, AXIS can detect the X-rays emitted by the passage of IMBHs within dense ISM environments. Such detections are crucial for understanding the demographics and evolution of IMBHs and the merging history of galaxies.

Author Contributions: Conceptualization: F.P., B.S., Y.N., N.C. and A.F.; software: F.P. and B.S.; writing—original draft preparation: F.P.; writing—review and editing: F.P., B.S., Y.N., N.C. and A.F. All authors have read and agreed to the published version of the manuscript.

Funding: This research received no external funding.

Data Availability Statement: Data is contained within the article.

Acknowledgments: F.P. acknowledges support from a Clay Fellowship administered by the Smithsonian Astrophysical Observatory. This work was also supported by the Black Hole Initiative at Harvard University, which is funded by grants from the John Templeton Foundation and the Gordon and Betty Moore Foundation. The authors kindly acknowledge the AXIS team for their outstanding scientific and technical work over the past year. This work results from several months of discussion in the AXIS-AGN SWG.

Conflicts of Interest: The authors declare no conflicts of interest.

References

1. Shakura, N.I.; Sunyaev, R.A. Reprint of 1973A&A....24..337S. Black holes in binary systems. Observational appearance. *Astron. Astrophys.* **1973**, *500*, 33–51.
2. Novikov, I.D.; Thorne, K.S. Astrophysics of black holes. In *Proceedings of the Black Holes (Les Astres Occlus)*; 1973; pp. 343–450. Available online: https://inspirehep.net/literature/1361968 (accessed on 10 May 2024).
3. Narayan, R.; Quataert, E. Black Hole Accretion. *Science* **2005**, *307*, 77–80. [CrossRef] [PubMed]
4. Fan, X.; Bañados, E.; Simcoe, R.A. Quasars and the Intergalactic Medium at Cosmic Dawn. *Annu. Rev. Astron. Astrophys.* **2023**, *61*, 373–426. [CrossRef]
5. Power, C.; Baugh, C.M.; Lacey, C.G. The redshift evolution of the mass function of cold gas in hierarchical galaxy formation models. *Mon. Not. R. Astron. Soc.* **2010**, *406*, 43–59. [CrossRef]
6. Begelman, M.C. Black holes in radiation-dominated gas—An analogue of the Bondi accretion problem. *Mon. Not. R. Astron. Soc.* **1978**, *184*, 53–67. [CrossRef]
7. Paczynski, B.; Abramowicz, M.A. A model of a thick disk with equatorial accretion. *Astrophys. J.* **1982**, *253*, 897–907. [CrossRef]
8. Abramowicz, M.A.; Czerny, B.; Lasota, J.P.; Szuszkiewicz, E. Slim accretion disks. *Astrophys. J.* **1988**, *332*, 646–658. [CrossRef]
9. Volonteri, M.; Rees, M.J. Rapid Growth of High-Redshift Black Holes. *Astrophys. J.* **2005**, *633*, 624–629. [CrossRef]

10. Sadowski, A. Slim Disks Around Kerr Black Holes Revisited. *Astrophys. J. Suppl. Ser.* **2009**, *183*, 171–178. [CrossRef]
11. Thorne, K.S. Disk-Accretion onto a Black Hole. II. Evolution of the Hole. *Astrophys. J.* **1974**, *191*, 507–520. [CrossRef]
12. Narayan, R.; Yi, I. Advection-dominated Accretion: A Self-similar Solution. *Astrophys. J.* **1994**, *428*, L13. [CrossRef]
13. Narayan, R.; Yi, I. Advection-dominated Accretion: Underfed Black Holes and Neutron Stars. *Astrophys. J.* **1995**, *452*, 710. [CrossRef]
14. Abramowicz, M.A.; Chen, X.; Kato, S.; Lasota, J.P.; Regev, O. Thermal Equilibria of Accretion Disks. *Astrophys. J.* **1995**, *438*, L37. [CrossRef]
15. Narayan, R.; McClintock, J.E. Advection-dominated accretion and the black hole event horizon. *New Astron. Rev.* **2008**, *51*, 733–751. [CrossRef]
16. Yuan, F.; Narayan, R. Hot Accretion Flows Around Black Holes. *Annu. Rev. Astron. Astrophys.* **2014**, *52*, 529–588. [CrossRef]
17. Yuan, F.; Quataert, E.; Narayan, R. Nonthermal Electrons in Radiatively Inefficient Accretion Flow Models of Sagittarius A*. *Astrophys. J.* **2003**, *598*, 301–312. [CrossRef]
18. Tchekhovskoy, A.; Narayan, R.; McKinney, J.C. Efficient generation of jets from magnetically arrested accretion on a rapidly spinning black hole. *Mon. Not. R. Astron. Soc.* **2011**, *418*, L79–L83. [CrossRef]
19. Kormendy, J.; Ho, L.C. Coevolution (Or Not) of Supermassive Black Holes and Host Galaxies. *Annu. Rev. Astron. Astrophys.* **2013**, *51*, 511–653. [CrossRef]
20. Greene, J.E.; Strader, J.; Ho, L.C. Intermediate-Mass Black Holes. *Annu. Rev. Astron. Astrophys.* **2020**, *58*, 257–312. [CrossRef]
21. Pacucci, F.; Mezcua, M.; Regan, J.A. The Active Fraction of Massive Black Holes in Dwarf Galaxies. *Astrophys. J.* **2021**, *920*, 134. [CrossRef]
22. Mezcua, M.; Siudek, M.; Suh, H.; Valiante, R.; Spinoso, D.; Bonoli, S. Overmassive Black Holes in Dwarf Galaxies Out to z 0.9 in the VIPERS Survey. *Astrophys. J. Lett.* **2023**, *943*, L5. [CrossRef]
23. Mezcua, M.; Pacucci, F.; Suh, H.; Siudek, M.; Natarajan, P. Overmassive black holes at cosmic noon: Linking the local and the high-redshift Universe. *Astrophys. J. Lett.* **2024**, *966*, L30. [CrossRef]
24. Pacucci, F.; Nguyen, B.; Carniani, S.; Maiolino, R.; Fan, X. JWST CEERS and JADES Active Galaxies at z = 4–7 Violate the Local $M_\bullet$-$M_\star$ Relation at $>3\sigma$: Implications for Low-mass Black Holes and Seeding Models. *Astrophys. J. Lett.* **2023**, *957*, L3. [CrossRef]
25. Pacucci, F.; Loeb, A. The Redshift Evolution of the $M_\bullet$–$M_\star$ Relation for JWST's Supermassive Black Holes at z > 4. *Astrophys. J.* **2024**, *964*, 154. [CrossRef]
26. Di Matteo, T.; Ni, Y.; Chen, N.; Croft, R.; Bird, S.; Pacucci, F.; Ricarte, A.; Tremmel, M. A vast population of wandering and merging IMBHs at cosmic noon. *Mon. Not. R. Astron. Soc.* **2023**, *525*, 1479–1497. [CrossRef]
27. Ricarte, A.; Tremmel, M.; Natarajan, P.; Quinn, T. Unveiling the Population of Wandering Black Holes via Electromagnetic Signatures. *Astrophys. J. Lett.* **2021**, *916*, L18. [CrossRef]
28. Weller, E.J.; Pacucci, F.; Hernquist, L.; Bose, S. Dynamics of intermediate-mass black holes wandering in the milky way galaxy using the illustris TNG50 simulation. *Mon. Not. R. Astron. Soc.* **2022**, *511*, 2229–2238. [CrossRef]
29. Weller, E.J.; Pacucci, F.; Ni, Y.; Chen, N.; Di Matteo, T.; Siwek, M.; Hernquist, L. Orbital and radiative properties of wandering intermediate-mass black holes in the ASTRID simulation. *Mon. Not. R. Astron. Soc.* **2023**, *520*, 3955–3963. [CrossRef]
30. Volonteri, M.; Begelman, M.C. Quasi-stars and the cosmic evolution of massive black holes. *Mon. Not. R. Astron. Soc.* **2010**, *409*, 1022–1032. [CrossRef]
31. Schleicher, D.R.G.; Palla, F.; Ferrara, A.; Galli, D.; Latif, M. Massive black hole factories: Supermassive and quasi-star formation in primordial halos. *Astron. Astrophys.* **2013**, *558*, A59. [CrossRef]
32. Ryu, T.; Tanaka, T.L.; Perna, R.; Haiman, Z. Intermediate-mass black holes from Population III remnants in the first galactic nuclei. *Mon. Not. R. Astron. Soc.* **2016**, *460*, 4122–4134. [CrossRef]
33. Portegies Zwart, S.F.; McMillan, S.L.W. The Runaway Growth of Intermediate-Mass Black Holes in Dense Star Clusters. *Astrophys. J.* **2002**, *576*, 899–907. [CrossRef]
34. Gürkan, M.A.; Freitag, M.; Rasio, F.A. Formation of Massive Black Holes in Dense Star Clusters. I. Mass Segregation and Core Collapse. *Astrophys. J.* **2004**, *604*, 632–652. [CrossRef]
35. Shi, Y.; Grudić, M.Y.; Hopkins, P.F. The mass budget for intermediate-mass black holes in dense star clusters. *Mon. Not. R. Astron. Soc.* **2021**, *505*, 2753–2763. [CrossRef]
36. González, E.; Kremer, K.; Chatterjee, S.; Fragione, G.; Rodriguez, C.L.; Weatherford, N.C.; Ye, C.S.; Rasio, F.A. Intermediate-mass Black Holes from High Massive-star Binary Fractions in Young Star Clusters. *Astrophys. J. Lett.* **2021**, *908*, L29. [CrossRef]
37. Fragione, G.; Kocsis, B.; Rasio, F.A.; Silk, J. Repeated Mergers, Mass-gap Black Holes, and Formation of Intermediate-mass Black Holes in Dense Massive Star Clusters. *Astrophys. J.* **2022**, *927*, 231. [CrossRef]
38. Alexander, T.; Natarajan, P. Rapid growth of seed black holes in the early universe by supra-exponential accretion. *Science* **2014**, *345*, 1330–1333. [CrossRef]
39. Natarajan, P. A new channel to form IMBHs throughout cosmic time. *Mon. Not. R. Astron. Soc.* **2021**, *501*, 1413–1425. [CrossRef]
40. Governato, F.; Colpi, M.; Maraschi, L. The fate of central black holes in merging galaxies. *Mon. Not. R. Astron. Soc.* **1994**, *271*, 317. [CrossRef]
41. Volonteri, M.; Haardt, F.; Madau, P. The Assembly and Merging History of Supermassive Black Holes in Hierarchical Models of Galaxy Formation. *Astrophys. J.* **2003**, *582*, 559–573. [CrossRef]

42. O'Leary, R.M.; Kocsis, B.; Loeb, A. Gravitational waves from scattering of stellar-mass black holes in galactic nuclei. *Mon. Not. R. Astron. Soc.* **2009**, *395*, 2127–2146. [CrossRef]
43. Greene, J.E.; Lancaster, L.; Ting, Y.S.; Koposov, S.E.; Danieli, S.; Huang, S.; Jiang, F.; Greco, J.P.; Strader, J. A Search for Wandering Black Holes in the Milky Way with Gaia and DECaLS. *Astrophys. J.* **2021**, *917*, 17. [CrossRef]
44. Seepaul, B.S.; Pacucci, F.; Narayan, R. Detectability of wandering intermediate-mass black holes in the Milky Way galaxy from radio to X-rays. *Mon. Not. R. Astron. Soc.* **2022**, *515*, 2110–2120. [CrossRef]
45. Ferrière, K.M. The interstellar environment of our galaxy. *Rev. Mod. Phys.* **2001**, *73*, 1031–1066. [CrossRef]
46. Igumenshchev, I.V.; Narayan, R.; Abramowicz, M.A. Three-dimensional Magnetohydrodynamic Simulations of Radiatively Inefficient Accretion Flows. *Astrophys. J.* **2003**, *592*, 1042–1059. [CrossRef]
47. Proga, D.; Begelman, M.C. Accretion of Low Angular Momentum Material onto Black Holes: Two-dimensional Magnetohydrodynamic Case. *Astrophys. J.* **2003**, *592*, 767–781. [CrossRef]
48. Perna, R.; Narayan, R.; Rybicki, G.; Stella, L.; Treves, A. Bondi Accretion and the Problem of the Missing Isolated Neutron Stars. *Astrophys. J.* **2003**, *594*, 936–942. [CrossRef]
49. Reynolds, C.S.; Kara, E.A.; Mushotzky, R.F.; Ptak, A.; Koss, M.J.; Williams, B.J.; Allen, S.W.; Bauer, F.E.; Bautz, M.; Bodaghee, A.; et al. Overview of the Advanced X-ray Imaging Satellite (AXIS). *arXiv* **2023**, arXiv:2311.00780.
50. Pesce, D.W.; Palumbo, D.C.M.; Narayan, R.; Blackburn, L.; Doeleman, S.S.; Johnson, M.D.; Ma, C.P.; Nagar, N.M.; Natarajan, P.; Ricarte, A. Toward Determining the Number of Observable Supermassive Black Hole Shadows. *Astrophys. J.* **2021**, *923*, 260. [CrossRef]
51. Marchesi, S.; Gilli, R.; Lanzuisi, G.; Dauser, T.; Ettori, S.; Vito, F.; Cappelluti, N.; Comastri, A.; Mushotzky, R.; Ptak, A.; et al. Mock catalogs for the extragalactic X-ray sky: Simulating AGN surveys with ATHENA and with the AXIS probe. *Astron. Astrophys.* **2020**, *642*, A184. [CrossRef]
52. Mushotzky, R.; Aird, J.; Barger, A.J.; Cappelluti, N.; Chartas, G.; Corrales, L.; Eufrasio, R.; Fabian, A.C.; Falcone, A.D.; Gallo, E.; et al. The Advanced X-ray Imaging Satellite. *Proc. Bull. Am. Astron. Soc.* **2019**, *51*, 107. [CrossRef]
53. Lusso, E.; Comastri, A.; Vignali, C.; Zamorani, G.; Brusa, M.; Gilli, R.; Iwasawa, K.; Salvato, M.; Civano, F.; Elvis, M.; et al. The X-ray to optical-UV luminosity ratio of X-ray selected type 1 AGN in XMM-COSMOS. *Astron. Astrophys.* **2010**, *512*, A34. [CrossRef]
54. Kruijssen, J.M.D.; Pfeffer, J.L.; Chevance, M.; Bonaca, A.; Trujillo-Gomez, S.; Bastian, N.; Reina-Campos, M.; Crain, R.A.; Hughes, M.E. Kraken reveals itself—The merger history of the Milky Way reconstructed with the E-MOSAICS simulations. *Mon. Not. R. Astron. Soc.* **2020**, *498*, 2472–2491. [CrossRef]
55. Karachentsev, I.D.; Makarov, D.I.; Kaisina, E.I. Updated Nearby Galaxy Catalog. *Astron. J.* **2013**, *145*, 101. [CrossRef]

Disclaimer/Publisher's Note: The statements, opinions and data contained in all publications are solely those of the individual author(s) and contributor(s) and not of MDPI and/or the editor(s). MDPI and/or the editor(s) disclaim responsibility for any injury to people or property resulting from any ideas, methods, instructions or products referred to in the content.